THE BELL SYSTEM TECHNICAL JOURNAL

DEVOTED TO THE SCIENTIFIC AND ENGINEERING ASPECTS OF ELECTRICAL COMMUNICATION

Volume 58 September 1979 Number 7

The EL2 Electret Transmitter: Analytical Modeling, Optimization, and Design

By J. C. BAUMHAUER, Jr. and A. M. BRZEZINSKI

(Manuscript received February 21, 1979)

We describe here the development of an EL2 Electret Transmitter that provides desirable attributes for use in hands-free-answer telephony and future electronic and special-purpose sets. The EL2 has lower sensitivity to spurious electromagnetic and mechanical signals than do existing magnetic transmitters. It offers lower dc power consumption, smaller size, and lower intrinsic noise and distortion than the carbon microphone. Formulation of an electro-mechano-acoustic electret model allows parameter optimization, in which side conditions on electrostatic stability and a prescribed transmit frequency response are adhered to. We show that higher sensitivities are possible with larger air film thickness, until the decreasing source capacitance becomes a limiting factor. Multiple diaphragm supports allow decreased film stress with no change in the stable electret charge or sensitivity. We describe theoretically a thermal stabilization procedure that minimizes long-range stress relaxation effects by accelerating viscoelastic changes. Based on film data, we project nominal sensitivity variations within ±1 dB over 20 years of service. In the design, metallized poly(tetrafluoroethylene) electret film is tensioned, supported, and clamped above a selectively metallized stationary electrode forming three cells acoustically and electrically in parallel. A preamplifier completes the subassembly, which is housed in a rectangular aluminum enclosure shielding the transducer. Typical EL2 parameters are −32 dBV/N/m² sensitivity at 1 kHz, 1 kΩ output impedance, 3.2 kHz response resonance frequency, and 2 to 16 V required dc supply.

I. INTRODUCTION

Electromagnetic transducers based on the modulation of a biasing magnetic field in an air film appeared as microphones (often referred to as transmitters in telephony), receivers, and loudspeakers very early in the development of telephony.[1,2] Today, this mechanism is employed in general-purpose U- and L-type telephone receivers in the Bell System. A smaller electromagnetic transducer, the AF1, was used as the electroacoustic transmitter in speakerphone modules until mid-1978. However, because of its operating principle, in recent years it was recognized to be inherently susceptible to an increasing incidence of spurious electromagnetic signals at customer locations. At the same time, interest was growing in a new telephone transmitter for electronic and special-purpose residential sets as well as for hands-free-answer features in business sets. The former residential applications generally require lower dc power consumption and smaller size than are typical of the variable-resistance granular carbon transmitter[3] such as the T-type used in general-purpose sets. Moreover, the carbon transmitter, being dependent upon periodic mechanical agitation, is not suitable as the stationary transmitter in hands-free-answer applications. These events encouraged Bell Laboratories development efforts[4] and the subsequent design of the EL2 Electret Transmitter. Compared to the AF1, the electret promised a greatly reduced sensitivity to electromagnetic as well as mechanical vibration interference. Its signal power efficiency is surpassed only by the carbon transmitter. However, compared to the latter, the electret could be used in applications where lower bias power consumption, smaller size, lower intrinsic noise and distortion, and the potential for longer service life were required.

A variable-capacitance transducer is based on the modulation of a biasing electrostatic field in an air film. In an electret, that field is provided by an "electret charge" distribution[5] typically implanted in, and near the surface of, a thin, solid, dielectric film abutting the air film. The externally biased condenser microphone was first demonstrated by A. E. Dolbear[6] in 1878, although E. C. Wente[7] was the first to develop a practical instrument in 1917 at the AT&T Research Laboratories. In 1928, S. Nishikawa and D. Nukiyama used a thick, wax plate electret element in building an early electret transducer.[8] In the United States, R. T. Rutherford was granted an electret microphone patent in 1935.[8] While the Japanese used wax electrets during World War II, their extremely low capacitance and unstable electret charge retention remained a problem.[8] In 1962, Sessler and West developed the electret-biased, polymer-film transducer[9,10] at Bell Laboratories. Made with charged thin Teflon† films, these microphones

† Registered trademark of E. I. DuPont de Nemours.

overcame the earlier limitations of self-biased units. Through the 1960s, large investments in the development and design of polymer-film electret microphones were made, largely outside telephony. Bell Canada introduced their electret transmitter design into an operator headset product in 1970[11] and later into a speakerphone. Recent efforts at Bell Laboratories culminated in initial Western Electric production shipments of the Bell System EL2 electret transmitter[12] in May 1977. It has now replaced the AF1 in the 4A Speakerphone and is being used as the stationary transmitter in a number of business sets for hands-free-answer services.

This paper covers the transducer device aspects of the EL2 development and design, while a companion article[13] will treat new technological aspects of the project. Here, analytical modeling and parameter optimization are first presented (Section II). Those results, coupled with physical, electrical, material, and telephone constraints are then shown applied in the physical design (Section III) to achieve performance and reliability objectives (Section IV).

II. ANALYTICAL MODELING AND OPTIMIZATION†

2.1 Transducer physics and model

Capacitance microphones are based on the modulation of a biasing dc electric field in a gas dielectric; the field in turn modulates the induced surface charge on an adjacent electrode. In the electret microphone (see Fig. 1), the biasing field in the air film is the result of a fixed "electret" surface charge[14] which may be considered trapped on an imaginary electrode at the surface of the polymer film adjacent the air film. Free charge is thus induced in the "stationary" electrode. Assuming a homogeneous isotropic linear solid dielectric and a one-dimensional electric field normal to the stationary electrode, an application of (*i*) the charge equation of electrostatics, (*ii*) Gauss's equation on the line integral of electric field, and (*iii*) jump conditions on the continuity of electric displacement[15] may be shown[16] to yield the electric field in the air film and the induced free surface charge on the stationary electrode as, respectively,

$$E_o^1 = (V_E + \sigma d/\epsilon)/(h^1 + d\epsilon_o/\epsilon),$$
$$\sigma_B^1 = \epsilon_o E_o^1 . \tag{1}$$

Here, ϵ and ϵ_o are the dielectric permittivity of the polymer and air films, respectively, $-\sigma$ is the negative electret surface charge per unit area, d and h^1 are the polymer and air film thickness, respectively, and an externally applied dc voltage V_E across the stationary and moving

† See appendix for partial list of symbols.

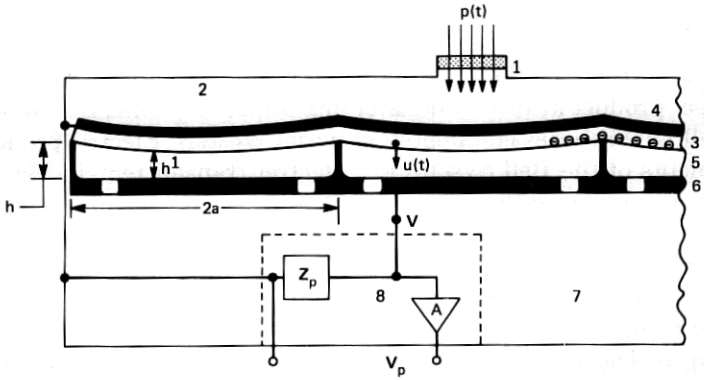

Fig. 1—Multicell electret transmitter: 1. Sound port and impedance material; 2. Front acoustic chamber; 3. "Electret-charged" polymer film diaphragm; 4. Diaphragm metallized electrode; 5. Air film; 6. Stationary electrode with holes; 7. Rear acoustic chamber; 8. Preamplifier.

diaphragm electrodes has been assumed presently, in addition to the electret self-bias. Meter-kilogram-second units have been employed. The electrostatic traction, Υ, exerted on the polymer film diaphragm is given by the normal surface component of the Maxwell electrostatic stress tensor[17] in the air film, i.e.,

$$\Upsilon = \epsilon_o (E_o^1)^2/2. \tag{2}$$

Since Υ, together with the polymer film membrane tension, will determine the biased diaphragm equilibrium displacement, it is clear from eqs. (2) and (1a) that electrostatically an electret bias charge σ of magnitude such that

$$\sigma d/\epsilon = V_E \tag{3}$$

is equivalent to an external voltage V_E present in a nonelectret capacitance (condenser) microphone. This equivalence, previously shown by Warren et al.[18] by employing energy considerations, can likewise be shown to hold for dynamic operation as first discovered by Sessler.[14] Henceforth, only a passive electret self-bias will be assumed present; that is, we take $V_E \equiv 0$ in eq. (1a). Of course, all results can easily be applied to capacitance microphones using the equivalence (3). It is noted that quantities representing the biasing electrostatic equilibrium (or intermediate) state are being designated with the superscript "1."

In Fig. 1, a multicell electret diaphragm supported by ribs, spaced at distance $2a$ and each of length $2b$, is shown in its equilibrium position. Identical individual cells operating acoustically and electrically in parallel are formed. A membrane diaphragm's effective "lumped parameter" mass, stiffness, and area (all per unit cell) may be written,

respectively,

$$M_e = \kappa \rho d a^2, \qquad K_e = \gamma S, \qquad A_e = \beta a^2 . \tag{4}$$

Here, ρ is the film mass per unit volume and S is the applied membrane force per unit edge, hereafter referred to as tension. For a rectangular diaphragm used in a capacitive transduction device, the constants may be shown to be appropriately based upon the average membrane displacement and are given by[16]

$$\kappa = \pi^4 \xi / 16\lambda, \qquad \gamma = \pi^2 \kappa / 4, \qquad \beta = 4\xi/\lambda, \tag{5}$$

where ξ is the number of cells formed and $\lambda = \xi 2a/2b$ is the prescribed overall diaphragm aspect ratio; the prescribed overall diaphragm area is then ξA_e. Relations (5) were derived assuming one-dimensional tension in the horizontal direction in Fig. 1, and with zero displacement at all boundaries surrounding each unit cell. Referring to the figure, the electrostatic displacement, w, of the effective rigid piston model is defined by

$$h^1 = h - w. \tag{6}$$

The input sound port and acoustic material act as a damped mass, M_F, of incompressible air, having effective area A_F and damping coefficient R_F, which add a degree of freedom to the system. When an acoustic signal $p(t)$ is impressed upon this mass, coupling to the diaphragm is effected through a front acoustic chamber stiffness K_F. Diaphragm motion is likewise influenced by the rear acoustic chamber stiffness K_R, thin air film damping[19] R_R, its own mechanical mass and stiffness, and air mass loading. Due to the inherently low capacitance of the combined cells, a preamplifier of high input impedance,

$$\mathbf{Z}_p = 1/(1/R_p + j\omega C_p), \tag{7}$$

and near-unity gain A is housed in the microphone rear acoustic chamber. Hereafter, a bold-face quantity denotes that it is to be considered complex.

2.2 Equations of motion and stability

One may show that the electrostatic potential energy stored in the dielectric/electrode system in Fig. 1 may be written in terms of σ, σ_B^1, d, and h^1. Energy and external work expressions for all mechanical, electrical, and acoustic elements may likewise be written. With these expressions, one can treat the coupled electrostatic-dynamic system by letting

$$\sigma_B^1 \rightarrow \sigma_B^1 + \tilde{\sigma}_B(t), \quad h^1 \rightarrow h^1 - u(t), \tag{8}$$

$\tilde{\sigma}_B$ being the "small" time-varying charge and u the small dynamic

diaphragm displacement. An application of Lagrange's equation yields the equations of motion[16]

$$\begin{bmatrix} PA_e \\ 0 \\ 0 \end{bmatrix} = \begin{bmatrix} \mathbf{Z}_K & 0 & \mathbf{Z}_F \\ \mathbf{Z}_M & -\chi & \mathbf{Z}_K \\ -\chi & \mathbf{Z}_e & 0 \end{bmatrix} \begin{bmatrix} \dot{\mathbf{U}} \\ \mathbf{I} \\ \dot{\mathbf{Y}} \end{bmatrix}, \tag{9}$$

where, assuming small dynamic fields superposed on a "large" electrostatic bias, we have used $u(t) \ll h^1$, $\tilde{\sigma}_B(t) \ll \sigma_B^1$. Above,

$$\chi = (\sigma d/\epsilon)/j\omega(h^1 + d\mu), \qquad \mu = \epsilon_o/\epsilon, \qquad j^2 = -1, \qquad \mathbf{Z}_K = -K_F/j\omega$$

$$\mathbf{Z}_F = (R_F + j\omega M_F)/\tau^2 - \mathbf{Z}_K, \qquad \tau = A_F/A_e, \qquad \mathbf{Z}_e = \mathbf{Z}_p + 1/j\omega C^1,$$

$$C^1 = \epsilon_o A_e \nu/(h^1 + d\mu), \qquad \mathbf{Z}_M = j\omega M_e + R_R + (K_e + K_R + K_F)/j\omega,$$

$$K_{F,R} = \rho_a c^2 A_e^2 \xi / v_{F,R}, \quad M_e \to M_e + (\tfrac{1}{3})\rho_a(v_F + v_R)/\xi. \tag{10}$$

In eqs. (9), P, $\dot{\mathbf{U}}$, $\mathbf{I} \equiv \dot{\tilde{\sigma}}_B A_e \nu$, and $\dot{\mathbf{Y}}\xi A_e$ are the steady-state complex amplitudes of the input sound pressure, piston diaphragm velocity, cell current, and sound port volume velocity, respectively, and χ is the electromechanical coupling coefficient. The factor ν is defined as that fraction of A_e metallized on the stationary electrode, ω is the circular frequency, v_F and v_R are the front and rear acoustic chamber volumes (v_R includes the volume of the stationary electrode holes), and ρ_a, c are the density of, and sound wave velocity in, air. Relation (10k) on M_e allows for the air mass loading on the diaphragm by the "gas spring" acoustic chambers. In addition, Lagrange's equations, due to equilibrium of the bias state, yield the electrostatic stability criterion

$$\eta - L/(1 - \eta)^2 = 0, \tag{11}$$

where, for a stable and physically realizable solution,

$$L \equiv (\sigma d/\epsilon)^2 \epsilon_o a^2 \beta \nu / 2\gamma S(h + d\mu)^3 \leqq 4/27,$$

$$\eta \equiv w/(h + d\mu) \leqq 1/3, \tag{12}$$

a well-known result.[20]

The open-circuit "cell sensitivity" and associated cell source impedance are defined, respectively, as

$$\mathbf{V} = \underset{Z_p \to \infty}{\text{Limit}} (\mathbf{Z}_p \mathbf{I})/P, \qquad \mathbf{Z}_s = (\mathbf{V}P)/\mathbf{I}|_{Z_p = 0}. \tag{13}$$

In the absence of small motional impedance terms evident near resonance, $\mathbf{Z}_s^{-1}$ can be shown to reduce to $j\omega C^1$, where C^1 is the cell capacitance in the electrostatic equilibrium state; see eq (10h). Of course, (13b) will be employed in calculations. The electret "transmit-

ter sensitivity" is given by

$$\mathbf{V}_p = \mathbf{V}[\mathbf{Z}_p/(\mathbf{Z}_p + \mathbf{Z}_s/\xi)]A, \tag{14}$$

where ξ accounts for the fact that the cells are in parallel, and A was defined following eq. (7). Before proceeding, it is noted from Griffin's work[19] that the thin air film damping R_R is proportional to $1/(h^1)^3$, and to the cube of the spacing between rows of stationary electrode holes in each cell as shown in Figs. 1 and 5. This degree of freedom over the magnitude of R_R will prove most helpful.

2.3 Optimization and EL2 design

In telephony, it is desirable that the transmit frequency response rises and peaks at the upper end of the telephone bandwidth, that is, between 3 and 4 kHz. This specification on frequency and level, which places a side condition on microphone design, may be approximated by allowing M_F and R_F, i.e., the sound port impedance, to vanish presently in the expression for $\mathbf{V}$. Then, finding the maxima of $|\mathbf{V}|$ with frequency in terms of the well-known dynamic magnification factor,[21] $\mathcal{M}(\omega)$, of a mass-spring-damper system can be shown to yield

$$\omega_d^2/\omega_n^2 = (1 - \mathcal{M}_M^{-2})^{1/2} = 1 - R_R^2/2M_e^2\omega_n^2, \tag{15}$$

where $\mathcal{M}_M$ is the maximum of $\mathcal{M}$ occurring at the damped resonance frequency ω_d, and the natural frequency is given by

$$\omega_n^2 = (K_e + K_R)/M_e. \tag{16}$$

Since $\mathcal{M}_M$ and ω_d will be prescribed, (15a) yields a side condition on ω_n. It is also seen from eq. (15b) that the desired $\mathcal{M}_M$ may be achieved by realizing the proper R_R as previously indicated. While the analytical optimization will be described more thoroughly in Ref. 16, most results are provided here. First, with stability criterion (12a) and side-condition (16), it may be shown that maximum $|\mathbf{V}|$ is achieved for $\omega_n^2 = K_e/M_e$, that is, $v_R = \infty$. A design at $K_e = K_R$ will be 3 dB below maximum $|\mathbf{V}|$, but will require lower film tension. This result is unlike that reported by Fraim et al.[22] where the frequency side condition was treated but not as an integral part of the optimization. Second, it may be shown that $|\mathbf{V}| \propto (h + d\mu)^{1/2}$ owing to a higher electrostatically stable electret charge level with increased h [see eqs. (11) and (12)] as seen in Fig. 2. However, since increasing h lowers the source capacitance, eq. (14) can yield a transmitter sensitivity which reaches a maximum with h, as seen. It may be shown from side condition (16) that

$$S \propto 1/\xi^2. \tag{17}$$

Then, in the stiffness-controlled region it follows that $|\mathbf{V}|$ is independ-

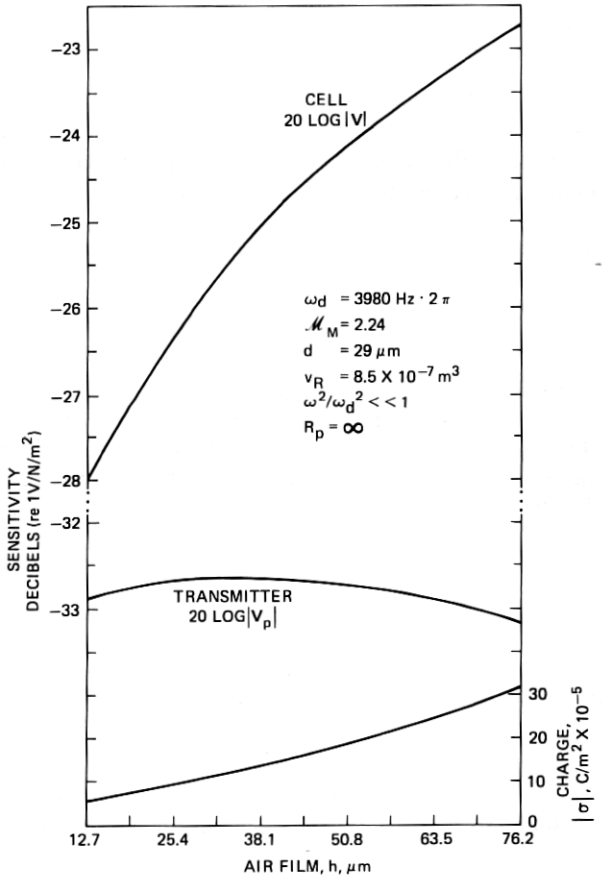

Fig. 2—One-day cell sensitivity, transmitter sensitivity, and corresponding stable electret charge vs air film thickness for a rectangular design. For all h, $S = 60.1$ N/m. No front chamber is present.

ent of ξ and thus cell size. Similarly, $|\mathbf{Z}_s|$ and $|\mathbf{V}_p|$ may be shown independent of ξ allowing relation (17) to be freely employed in keeping film stress levels below strength limitations by increasing ξ.

The design approach is now to use condition (16) to determine S for a given geometry. Then constraint (12a) determines the stable charge level possible. Such data were obtained for the EL2 for $\omega^2/\omega_d^2 \ll 1$ while iterating parameters such as d, h and v_R. In applying (12a), the upper bound on L, i.e., 4/27, was reduced to $\zeta(4/27)$ to allow margin for (*i*) worst-case tolerances expected, (*ii*) anticipated aging effects, and (*iii*) a safety factor related to extreme service conditions, modeling assumptions, etc. Item (*ii*) is discussed later. The following values,

descriptive of the EL2, were used to generate Fig. 2:

$$\omega_d = 2\pi(3980 \text{ Hz}),\dagger \quad \mathcal{M}_M = 2.24,\dagger \quad \xi A_e = 7.3 \times 10^{-5} \text{ m}^2,$$
$$\lambda = 1.74, \quad \xi = 3, \quad \nu = 0.73, \quad d = 29 \ \mu\text{m},$$
$$v_R = 8.5 \times 10^{-7} \text{ m}^3,$$
$$\zeta = 0.114, \quad \rho = (2.23 \times 10^3 + 38.6 \times 10^{-4}/d) \text{ kg/m}^3,$$
$$\epsilon = 2.08\epsilon_o, \quad A = 0.9, \quad C_p = C_{\text{in}} + C_{\text{stray}} = (5 + 6) \text{ pF}. \quad (18)$$

The second term in eq. (18*j*) on ρ is added to the EL2 polymer film density to account for the metallized electrode mass (film and metallization are described in Section III), and ϵ_o, ρ_a, and c are well known. For all h in Fig. 2, condition (16) yielded tension $S = 60.1$ N/m. Curves such as those in Fig. 2 together with additional physical, material, and electrical constraints allowed optimum final parameters such as h, d, and v_R to be chosen. With the parameters in eq. (18) and choosing $h = 36.1$ μm, Fig. 2 gives $\sigma = 13 \times 10^{-5}$ C/m^2 ($\sigma d/\epsilon = 204$ volts) for the EL2.

2.4 Thermal stabilization and EL2 performance

Given the above EL2 design parameters, we find that $h^1 = 35.2$ μm and $R_R = 0.032$ Ns/m which, together with cell geometry, yield[19] the required spacing between rows of holes in the stationary electrode. Then the transmitter performance including its sound port acoustic impedance[23] influence is seen in Fig. 3, where we have used for the EL2

$$R_p = 10^8 \text{ ohms}, \quad v_F = 0.7 \times 10^{-7} \text{ m}^3, \quad A_F = 1.72 \times 10^{-6}/\xi \text{ m}^2,$$
$$R_F = 0.4 \ \rho_a\phi/\xi + 2.53 \times 10^{-6}\rho_a(\omega\phi)^{1/2}/\xi \text{ Ns/m},$$
$$M_F = 2.21 \times 10^{-9}\rho_a/\xi \text{ kg}, \quad (19)$$

ϕ being the kinematic viscosity of air. The calculated response is seen to match that typically measured quite favorably across the telephone bandwidth. The response, influenced by input acoustics, peaks at about 3080 Hz and $|\mathbf{V}_p|$ at 1 kHz and ξC^1 are -31.8 dBre 1 $V/\text{N/m}^2$ and 9.6 pF, respectively. Above the frequency of peak response (associated with the first diaphragm resonance), the results begin to differ due to the single degree-of-freedom model used for the continuous diaphragm.

To this point, we have ignored tension and electret charge variation with time; accordingly, all previous results are referred to 1 day past manufacture, as represented in Figs. 2 and 3. However, the viscoelastic polymer film undergoes stress relaxation and/or creep under load. Similarly, extensive investigation has been conducted on electret charge retention at Bell Laboratories and will be reviewed in a com-

† Prescribed in the absence of sound port impedance.

panion article.[13] Here, we simply give a curve fit for the assumed EL2 electret charge retention at room conditions normalized to the 1-day level, $\sigma[1]$:

$$\sigma(t)/\sigma[1] = \sum_i \Gamma_i e^{-t/\delta_i}, \quad (600\ s \leqq t \leqq 20\ \text{yrs}),$$

$$\Gamma_i \rightarrow \begin{bmatrix} 0.954 \\ 0.039 \\ 0.001 \\ 0.004 \\ 0.003 \\ 0.005 \end{bmatrix}, \qquad \delta_i \rightarrow \begin{bmatrix} 9.66 \times 10^{11} \\ 1.08 \times 10^{9} \\ 2.37 \times 10^{7} \\ 3.81 \times 10^{6} \\ 2.50 \times 10^{5} \\ 1.03 \times 10^{4} \end{bmatrix} s. \tag{20}$$

Data indicate the initial electret charge to be about 1 percent above $\sigma[1]$, which will be employed here. Since $\sigma/\sigma[1]$ is only down to 0.97 at 20 years, it is not surprising that the diaphragm tension relaxation will be of far greater impact. Recently, Wang and Matsuoka[24] studied the viscoelastic behavior of metallized annealed EL2 film. Through time-temperature superposition, they obtained a reduced relaxation modulus vs reduced time over a 500-year period at room temperature (using 18,000-s high temperature isotherms-ambient to 75°C). Using a generalized Maxwell model,[25] their result for the room temperature relaxation modulus is here expressed numerically by

$$\mathcal{G}^o(t) = \sum_i \mathcal{G}_i e^{-t/\iota_i}, \quad (600\ s \leqq t \leqq 500\ \text{yrs}),$$

$$\mathcal{G}_i \rightarrow \begin{bmatrix} 30.11 \\ 3.61 \\ 4.04 \\ 4.42 \\ 4.97 \\ 7.03 \end{bmatrix} \times 10^7\ \text{N/m}^2, \qquad \iota_i \rightarrow \begin{bmatrix} 1.14 \times 10^{11} \\ 1.59 \times 10^{9} \\ 1.88 \times 10^{8} \\ 6.36 \times 10^{6} \\ 2.38 \times 10^{5} \\ 6.48 \times 10^{3} \end{bmatrix} s, \tag{21}$$

where superscript "o" denotes room temperature. To their Arrhenius plot of the temperature shift factor a_T, the Arrhenius equation,

$$\ln a_T = 25{,}530[1/(T + 273) - 1/(T^o + 273)], \tag{22}$$

has here been fit, where T is temperature in °C, and $T^o = 22.7$ °C.

In EL2 manufacture, the diaphragm undergoes a fixed stress $\bar{\sigma}^M$ for a short duration, $t = 0$ to $\bar{t}$, during which time the material creeps to strain $\bar{\epsilon}^M$. At time $\bar{t}$, the film diaphragm is clamped permanently at strain $\bar{\epsilon}^M$. Stress relaxation in accordance with the decreasing modulus then ensues. While $\bar{\sigma}^M$ could be chosen such the proper membrane tension, S, and hence frequency response previously prescribed at 1 day were obtained, unsatisfactory increases in sensitivity and decreases in resonance frequency would occur during, say, a 20-year service life.

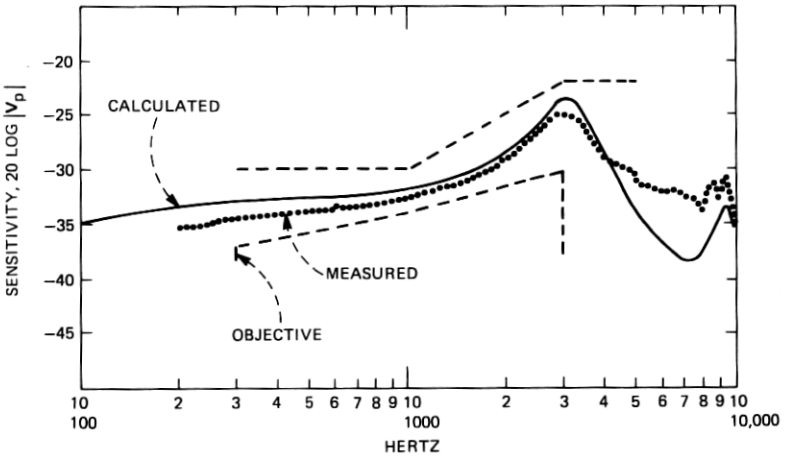

Fig. 3—Typical EL2 frequency response one day after assembly (following thermal stabilization), at room temperature.

For this reason,[26] a "thermal stabilization" procedure has been developed whereby the electret devices are placed at high temperature T^* for duration $\Delta t = t_2 - t_1$ where $\bar{t} \ll t_1 < t_2 \leqq 86{,}400\ s$ (1 day). While the mechanics of the resulting thermoviscoelastic problem are only sketched below, the reader may refer to Ref. 16 for more details. For a thermorheologically simple viscoelastic material undergoing "small" strain, the following linear constitutive equation holds[27]

$$\sigma^M(t) \equiv \hat{\sigma}^M(\theta) = \int_0^\theta \mathscr{G}^o(\theta - \theta') \frac{\partial \epsilon^M(\theta')}{\partial \theta'} d\theta',$$

$$\theta(t) \equiv \int_0^t 1/a_T \, dt, \tag{23}$$

where t is the real, and θ the reduced, time. For $t \gg \bar{t}$, it may be shown that the creep between $t = 0$ and $\bar{t}$ may be viewed as a step in strain of magnitude $\bar{\epsilon}^M$ at $t = 0$. From the convolution integral (23a), it may be shown using the Dirac-delta function and Laplace transforms that

$$\sigma^M(t) = \hat{\sigma}^M(\theta) = \bar{\epsilon}^M \mathscr{G}^o(\theta), \qquad t \gg \bar{t}. \tag{24}$$

Now, for $\bar{t} \ll t \leqq t_1$, $\theta = t$ and eq. (24) yields a well-known result.[28] During stabilization, eq. (23b) gives $\theta = t_1 + (t - t_1)/a_T(T^*)$, which is the basis for time-temperature superposition.[29] For the service life, $t \geqq t_2$,

$$\theta = t_1 + (t - t_2) + \Delta t/a_T(T^*). \tag{25}$$

At 1 day, the stress $\sigma^M = S/d$ is prescribed as can be seen from eqs.

(15), (16), and (4b)—see the argument following eq. (16). Thus, $\bar{\epsilon}^M$ may be determined from eqs. (24) and (25). In a manner similar to that used in obtaining eq. (24), it can be shown that the actual step change in $\bar{\sigma}^M$ at $t = 0$ yields

$$\epsilon^M(t) = \bar{\sigma}^M J^o(t), \qquad 0 < t \leqq \bar{t}. \tag{26}$$

With the creep compliance $J^o(\bar{t})$ known, we can then find from eq. (26) the required $\bar{\sigma}^M$ that must be applied to the film for duration $\bar{t}$ to achieve the desired 1-day tension following stabilization. Microphone performance for all $t \gg \bar{t}$ (i.e., during the service life) is thus independent of the choice of a $(\bar{t}, \bar{\sigma}^M)$ pair satisfying eq. (26). However, since the creep compliance increases more rapidly with time initially, manufacturing tolerances on $\bar{t}$, to maintain a given (acceptable) variance on σ^M for all $t \gg \bar{t}$, are less restrictive for larger $\bar{t}$. Desiring time-independent transmitter performance through the service life, the following parameters were chosen for the EL2: $T^* = 60°C$, $\Delta t = (2/3$ day), and $t_2 = (1$ day), yielding $\bar{\epsilon}^M = 0.65$ percent. Then, for for $\bar{t} = 60$ s, we use[24] $J^o(\bar{t}) = 10.6 \times 10^{-6}$ m^2/N and obtain the EL2 initial stress $\bar{\sigma}^M = 4.2 \times 10^6$ N/m^2 or tension, 122 N/m (more than twice the 1-day level), to be applied. Note that $\bar{\sigma}^M$ could be lowered by increasing $\bar{t}$. It is interesting that at 1 day, $\theta \simeq$ (29 years), that is, the equivalent of 29 years of room temperature relaxation has been effected. Now, with time variations in both eqs. (20) and (24) present, quantities like h^1, R_R, and K_e change accordingly, and the results in Fig. 4 are obtained; EL2 performance during the service life has been "stabilized." The 1-kHz transmitter

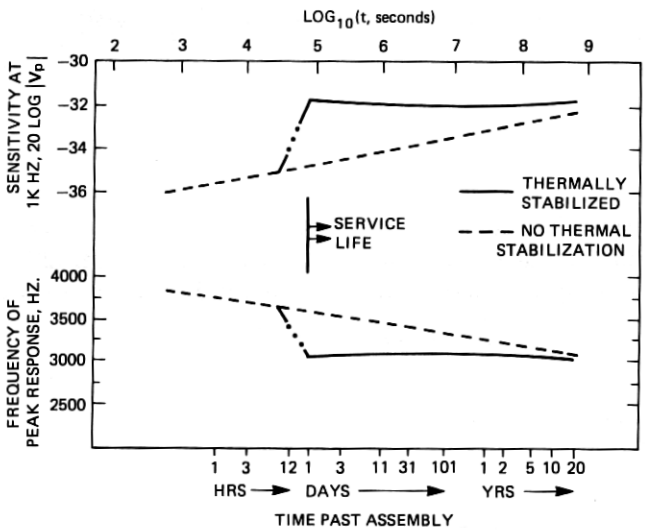

Fig. 4—Predicted EL2 sensitivity at 1 kHz and frequency of peak response level vs time at room temperature, stabilized at 60°C for 16 hours.

sensitivity is seen to drop very slightly during the first year due to minor but dominant charge decay assumed, after which time slight tension relaxation causes $|V_p|$ to rise and the resonance frequency to decline slightly.

III. PHYSICAL DESIGN

3.1 Constraints and objectives

The physical design of the EL2 electret transmitter was guided by the following factors: potential applications, reliability, and manufacturability. The primary application for the new electret microphone has been the replacement of the AF1 in the 680-type transmitter module used with the 4A Speakerphone. This application dictated physical constraints based on the existing module configuration. The size of the AF1 was an upper bound on that of the EL2. Electrical compatibility with other expected applications was also a major influence on the impedance and dc power requirements for the microphone. The low cell capacitance results in a combined cell source impedance ($\mathbf{Z}_s/\xi$) of 16 MΩ at 1 kHz. This high impedance necessitates the use of an internal preamp intimately associated with the cells to reduce loading of the output signal (**V**), and to minimize external electromagnetic field pickup. Potential use in line-powered applications required the preamplifier to be operational down to a supply voltage of 2 volts. Performance objectives were also stipulated to insure satisfactory operation in all anticipated applications. Electroacoustic conversion efficiency, frequency response, and mechanical and electromagnetic interference sensitivity were some of the operational characteristics specified.

The optimized parameters generated with the analytical model [see eqs. (18) and (19) for most physical design parameters] provided a framework for the physical design. The ultimate configuration reflects model results that were in turn influenced by physical, material, and telephone constraints. A major effort was made to insure simplicity and ease of assembly while stressing environmental reliability and long life. Twenty years service within an operating temperature range of −23°C to +49°C was the overall design objective.

3.2 Description

3.2.1 Subassembly

The heart of the microphone is the subassembly or "cartridge," shown in the exploded view in Fig. 5. The diaphragm is positioned and tensioned across the face of the backplate between the shim and clamping plate. The spring clip clamps these parts against the top of the backplate while holding the preamplifier in position on the underside. The backplate is the nucleus of this structure with the other parts

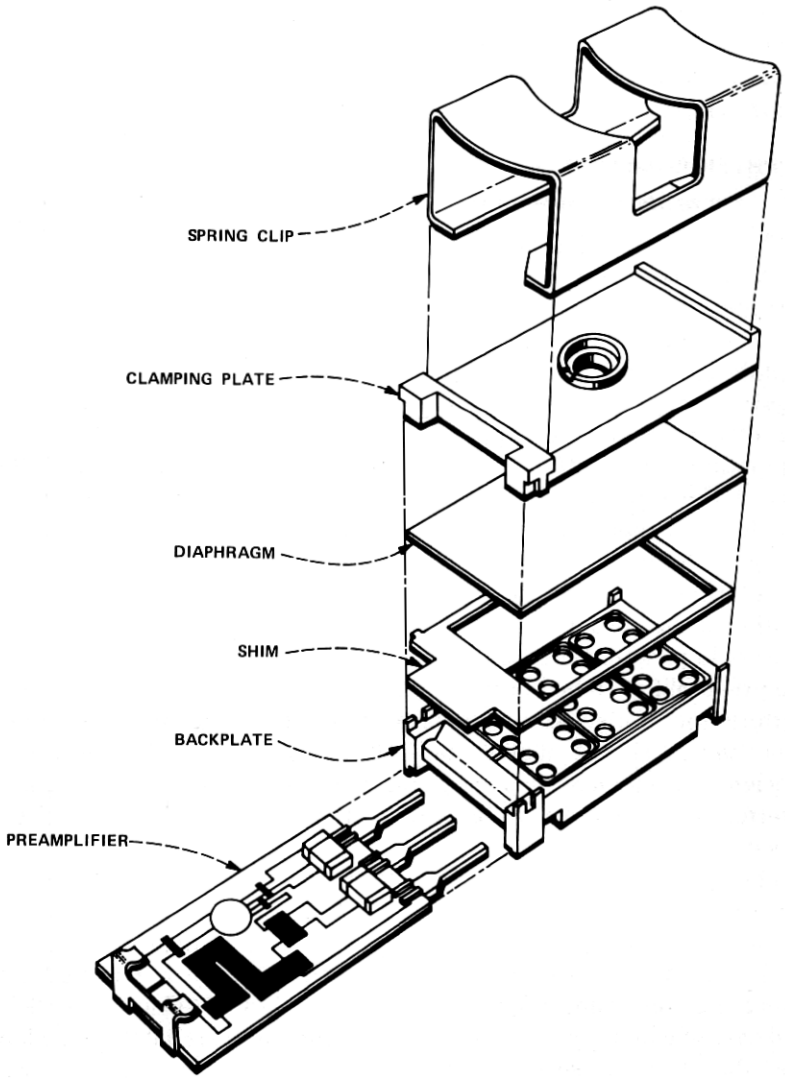

Fig. 5—EL2 subassembly.

assembled to it. An electroplatable grade of acrylonitrile butadiene styrene (ABS) is used to mold the backplate to facilitate selective metallization of the three microphone cell areas located on its upper surface. These conductive areas, which are electrically common, serve as the stationary electrode of the microphone configuration. A small diaphragm support rib 36 μm high (h) surrounds each metallized cell area. These supports are unmetallized to reduce stray capacitance. The diaphragm resting on these ribs creates the air film (h^1) between

the flexible diaphragm and the stationary electrode. The sensitivity of the microphone output to changes in this air film necessitates the use of precision molding techniques to maintain dimensional control of rib height to within ±5 μm (±0.0002 in). The holes through the backplate couple the air film under the diaphragm to the rear acoustic chamber and are spaced at a distance to effect proper air film damping in accordance with the model in Section II. They are located in rows at the outer edges of the cells adjacent to the ribs. This maximizes the amount of continuous electrode area (νA_e) in the center region where the greatest diaphragm displacement (u) occurs.

The preamplifier is a conventional source follower configuration with a JFET transistor and two thick film resistors on a ceramic substrate providing an effective impedance transformation and a voltage gain of −1 dBV. The input impedance ($\mathbf{Z}_p$) is approximately 100 M ohms resistance in parallel with about a 5-pF junction, and 6-pF stray capacitance. The output impedance is nominally 1 kilohm. A contact spring soldered to one end of the substrate provides electrical continuity from the stationary electrode on the backplate to the input of the amplifer circuit, while mechanically clipping the preamp to the backplate. Three leads extending from the opposite end of the substrate provide for electrical bias, output, and common connections to the assembled microphone. Two small chip capacitors bridge these leads on the substrate to provide RFI suppression.

The electret diaphragm material is a 29-μm thick, stress-relieved, cast, poly(tetrafluoroethylene) (PTFE) film. It is metallized on one side with a titanium flash approximately 100 Å thick under 2000 Å of evaporated gold.[13] The metallized side of the film functions as the movable electrode in the microphone. This particular Teflon film was selected for its superior charge retention characteristics. It is electrostatically charged to approximately 13×10^{-5} C/m^2 to provide the electric field (E_o^1) in the microphone assembly air film. The charge ($-\sigma$) on the polymer film eliminates the need for the external dc bias required in conventional condenser microphones. The diaphragm is tensioned longitudinally under fixed load $S = 122$ N/m for duration $\bar{t} = 60$ sec minimum prior to clamping it in the relative position indicated, and with the metallized side opposite the air film. The nominal value of $\bar{t}$ chosen is influenced by two primary considerations. The duration of $\bar{t}$ should be maximized to minimize its tolerance stringency [see the discussion following eq. (26)], whereas it should be minimized for the sake of manufacturing expediency.

A thin Mylar† shim is sandwiched between the backplate and

† Registered trademark of E. I. DuPont de Nemours.

clamping plate along with the diaphragm film. It provides a relatively compliant surface against which to clamp the film. "Hard" clamping the diaphragm without a shim would result in nonuniform clamping pressure, causing nonuniform tension across the width of the film. The tab on the end of the shim provides electrical insulation between the preamp contact spring and the enclosure in the final assembly.

The clamping plate is a metallized precision molded piece part which is indexed on the backplate and clamps the pretensioned diaphragm in position across the cell area. Both the clamping plate and backplate are molded from the same grade of ABS material so as to have a similar thermal expansion coefficient. This coefficient also approximates that of the electret film. The clamping plate is metallized to provide electrical continuity from the metallized side of the electret film to the spring clip, which is connected directly to the common terminal on the preamp.

The phosphor bronze spring clip maintains a compressive spring force of approximately 20 N on the assembled parts to keep the diaphragm properly tensioned. This force is sufficiently large to prevent slippage of the diaphragm in the cartridge assembly, but is limited to avoid overstressing and causing cold flow of the plastic parts. The clip also provides electromagnetic shielding by surrounding most of the subassembly and being electrically connected to the preamp common terminal. After clamping with the spring clip, the subassembly is a working microphone configuration. The spring clip design permits easy disassembly to facilitate repair or reassembly if required prior to final assembly.

The completed cartridge assembly is thermally stabilized, which involves "soaking" the units at an elevated temperature of 60°C for a period of 16 hours to accelerate the diaphragm stress relaxation. This preaging treatment results in a more uniform and stable product (see Fig. 4). Preliminary testing is done after stabilization to evaluate microphone performance prior to final assembly.

3.2.2 Final assembly

Final assembly involves ferruling the pretested subassembly into a rectangular aluminum enclosure and back cover. A stainless steel woven wire acoustic screen is included in front of the subassembly and a gasket across the back, as shown in Fig. 6. The screen, in conjunction with the input sound port, provides acoustic impedance elements R_F and M_F which modify the frequency response. The wire screen also serves as a dirt shield across the input sound port. The gasket provides electrical insulation between the preamp and back cover and functions as a shock-absorbing element in the microphone assembly. The external aluminum enclosure is electrically connected to the common ter-

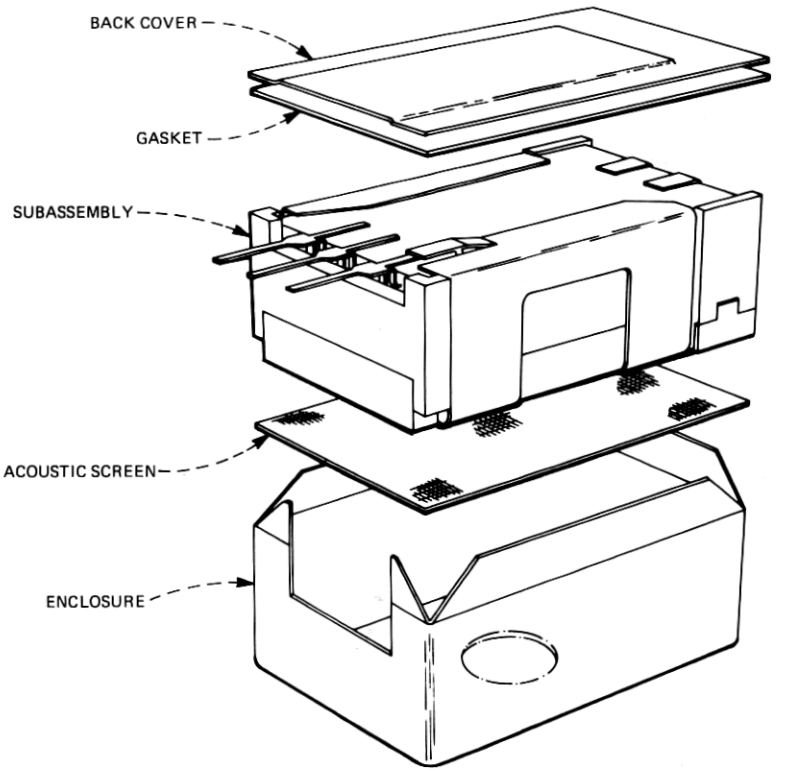

Fig. 6—EL2 final assembly.

minal on the preamp, thereby providing additional electromagnetic shielding. Acoustic leaks around the leads are sealed, and the complete unit is tested according to the final requirements. A cross section of the completed EL2 microphone is illustrated in Fig. 7 to provide an overall perspective of the assembly, which is 18 by 12 by 7.6 mm in depth.

IV. MICROPHONE PERFORMANCE

4.1 Performance characteristics

The EL2 operates on a bias supply of 2 to 16 V while drawing about 150 μA. Figure 3 shows a typical measured frequency response of the telephone transducer compared to the calculated result from the model. The response is relatively flat in the lower frequency stiffness-controlled region and rises about 7 dB to the resonance peak at 3200 Hz, above which the level falls off rapidly. The typical electroacoustic sensitivity at 1 kHz is -32.0 dBV/N/m^2. Model results show that the output signal level is altered by (uncompensated) changes in a number

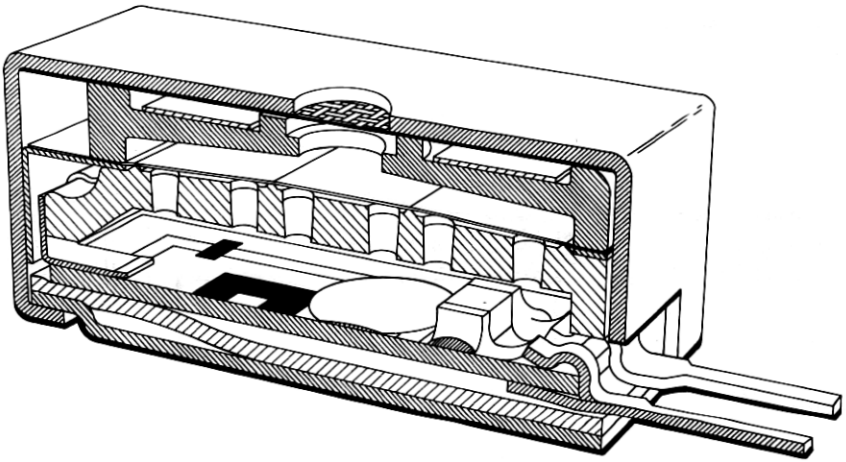

Fig. 7—EL2 Transmitter Unit.

of the basic microphone parameters. For example, the variation of output voltage versus charge for this microphone configuration is given by 0.7 dBV/10^{-5}C/m^2. This relationship was verified both analytically and empirically. EL2 sensitivity will also vary with changes in the air film thickness in accordance with the gradient −1.4 dBV/5μm, which substantiates the need for precision molding of the diaphragm support ribs. The microphone output variation with applied tension is given by −0.5 dBV/8N/m. The resonance frequency also varies with tension according to the ratio of 100 Hz/8N/m. It must be pointed out that these coefficients, which are linear approximations, apply only for minor variations about the nominals specified for the basic parameters.

The vibration sensitivity of the microphone is < −40 dB re 1 V/g at 1000 Hz. The EL2 "signal voltage to spurious mechanical noise voltage" ratio is about 20 dB greater than that of the AF1 microphone. This improved vibration isolation is acquired due to the relatively low mass of the electret diaphragm. The RFI sensitivity is < −75 dB re 1 V in a 10 V/m field from 0 to 300 MHz. The hum or low-frequency electromagnetic pickup sensitivity is < −95 dB re 1 V/gauss at 60 Hz. The hum interference rejection of the electret is 35 dB better than that of the AF1. In general, the electret microphone successfully met all the performance objectives initially outlined and performs well as a replacement for the AF1 in the 4A Speakerphone.

4.2 Reliability

The ruggedness and reliability of the EL2 design have been established by tests[30] which included mechanical and thermal shock, vibra-

tion, and combinations of temperature and humidity. The small changes which occurred during the course of the study tests had minimal effect on overall performance. The output was found to vary slightly as a function of temperature at a rate of 0.045 dB/°C.[30] This is a reversible effect, resulting in no permanent change in output upon return to ambient temperature. The charge retention of the EL2 electret film, found to be very stable, is discussed in detail in a companion article.[13] Moreover, earlier studies over 800 days of testing compared sensitivity variations (aging) of numerous commercial and Bell Labs' prototype electret microphones to transducers employing other mechanisms including granular carbon, electromagnetic, and piezoelectric. The aging conditions ranged between 25°C/40% R.H. and 65°C/90% R.H. The electret devices performed comparably to the other types of microphones in these tests.

V. SUMMARY

An EL2 electret transmitter has been developed which provides lower sensitivity to spurious electromagnetic and mechanical signals than the AF1 magnetic transmitter it has replaced in the 4A Speakerphone. It offers lower dc power consumption, smaller size, and lower intrinsic noise and distortion than the carbon transmitter. These attributes make it a strong candidate to replace the carbon transmitter in future electronic and special-purpose sets.

An electro-mechano-acoustic model of an electret transmitter governing its coupled electrostatic/dynamic operation has allowed EL2 parameters such as air film thickness, number of cells, and acoustic chamber volume to be collectively optimized. It is shown that, within bounds, sensitivity can actually be raised by designing with increased air film thicknesses. The analysis is novel in consistently treating a side condition governing the prescribed response resonance characteristics as an integral part of the optimization. Also, a thermal stabilization procedure used to minimize the effects of long-term stress relaxation (accompanied by charge decay) is described theoretically and optimized. Virtually constant sensitivity over the service life is shown possible.

These results, coupled with physical, material, and application constraints, are shown applied in the physical design to achieve desired performance and reliability. A metallized Teflon electret film is tensioned, supported, and clamped above a selectively metallized stationary electrode forming three cells acoustically and electrically in parallel. A preamplifier and input sound port complete the subassembly, which is then tested and housed in a rectangular aluminum enclosure, electrically shielding the transducer. The nominal EL2 electroacoustic sensitivity, output impedance, response resonance frequency, and re-

quired dc supply are -32 dBV/N/m^2, 1 kΩ, 3200 Hz, and + 2 to 16 V, respectively. The response is relatively flat in the low-frequency stiffness-controlled region. A 3-dB cutoff occurs below 100 Hz.

For completeness, note that the EL2 is described here as it existed in the initial design and field trial units and does not reflect minor changes as a result of manufacturing experience. A companion article[13] will treat the new technological aspects of the EL2.

VI. ACKNOWLEDGMENTS

The authors are thankful to J. E. Warren for stimulating discussions regarding the mathematical model and helpful suggestions during the overall EL2 design effort. S. R. Whitesell contributed to final design modifications, and R. S. Ball to meaurements required in support of EL2 introduction to manufacture. T. T. Wang shared ideas regarding implications of the viscoelastic nature of the film and obtained required film data.

APPENDIX

Partial List of Symbols

$-\sigma$	Negative electret surface charge per unit area.
h^1	Air film thickness in the electrostatic state.
h	Rib height.
d	Polymer film thickness.
$\mu = \epsilon_0/\epsilon$	Inverse of relative permittivity.
M_e, A_e, K_e	Diaphragm effective mass, area, and stiffness per unit cell.
S	Membrane diaphragm's applied force per unit edge (tension).
ξ	Number of diaphragm cells.
v_R, K_R	Rear acoustic chamber volume, stiffness.
R_R	Air film damping coefficient
ν	That fraction of A_e metallized on the rear electrode.
w, $u(t)$	Diaphragm electrostatic and dynamic displacement.
V, Z_s	Cell open-circuit sensitivity and source impedance.
C^1	Electrostatic cell capacitance.
$Z_p = (1/R_p + j\omega C_p)^{-1}$	Preamplifier input impedance.
V_p	Transmitter (microphone) sensitivity.
ω_n, ω_d	Diaphragm natural and damped resonance frequency (in absence of front chamber).

$\mathcal{M}_M$	Maximum of the dynamic magnification factor (in absence of front chamber).
$\mathscr{G}^\circ(t)$	Room temperature mechanical relaxation modulus of the metallized film diaphragm.
$\sigma^M(t)$, $\epsilon^M(t)$	Diaphragm stress and strain.
t, θ	Real and reduced time.
$\bar{t}$	Time duration of diaphragm creep prior to clamping.
$\bar{\sigma}^M$, $\bar{\epsilon}^M$	Diaphragm stress and strain at time $t = \bar{t}$.

REFERENCES

1. Alexander Graham Bell, "Researches in Telephony," Proc. Am. Acad. Arts Sci., *12* (1877), pp. 1–10.
2. C. Flannagan, R. Wolf, and W. C. Jones, "Modern Theater Loud Speakers and Their Development," J. Soc. Mot. Pict. Eng., *XXVIII*, No. 3 (May 1937), pp. 246–263.
3. F. S. Goucher, "The Carbon Microphone," B.S.T.J., *13*, No. 2 (April 1934), pp. 163–194.
4. J. E. Warren, J. F. Hamilton, and A. M. Brzezinski, "Capacitance Microphone Dynamic Membrane Deflections," J. Acoust. Soc. Am., *54*, No. 5 (1973), pp. 1201–1213.
5. H. J. Wintle, "Introduction to Electrets," J. Acoust. Soc. Am., *53*, No. 6 (June 1973), pp. 1578–1588.
6. J. K. Hilliard, "Electroacoustics to 1940," J. Acoust. Soc. Am., *61*, No. 2 (February 1977), pp. 267–273. See Section VII.
7. E. C. Wente, "A Condenser Transmitter as a Uniformly Sensitive Instrument for the Absolute Measurement of Sound Intensity," Phys. Rev., *10* (July 1917), pp. 39–63.
8. G. M. Sessler and J. E. West, "Electret Transducers: A Review," J. Acoust. Soc. Am., *53*, No. 6 (June 1973), pp. 1589–1599.
9. G. M. Sessler and J. E. West, "Condenser Microphone with Solid Dielectric," J. Audio Eng. Soc., *10*, No. 3 (July 1962), pp. 212–215.
10. G. M. Sessler and J. E. West, "Self-Biased Condenser Microphones with High Capacitance," J. Acoust. Soc. Am., *34*, No. 11 (November 1962), pp. 1787–1788.
11. C. W. Reedyk, "Noise-Cancelling Electret Microphone for Lightweight Head Telephone Sets," J. Acoust. Soc. Am., *53*, No. 6 (June, 1973), pp. 1609–1615.
12. J. C. Baumhauer, Jr., A. M. Brzezinski, J. E. Warren, and S. R. Whitesell, "Electroacoustic Transducer...," U.S. Patent 4,046,974, applied for October 1976, issued September 1977.
13. S. P. Khanna and R. L. Remke, Bell Laboratories, to be published.
14. G. M. Sessler, "Electrostatic Microphone with Electret Foil," J. Acoust. Soc. Am., *35*, No. 9 (September 1963), pp. 1354–1357.
15. J. C. Baumhauer and H. F. Tiersten, "Nonlinear Electroelastic Equations for Small Fields Superposed on a Bias," J. Acoust. Soc. Am., *54*, No. 4 (1973), pp. 1017–1034. See eqs. (4), (6), (7), and (20a).
16. J. C. Baumhauer, Jr., "Modeling and Analysis of Electret Microphones—An Example in Telephony," to be published.
17. H. F. Tiersten, "On the Nonlinear Equations of Thermoelectroelasticity," Int. J. Engng. Sci., *9* (1971), pp. 587–604. See eq. (3.19).
18. J. E. Warren, J. F. Hamilton, and A. M. Brzezinski, "Capacitance Microphone Static Membrane Deflections," J. Acoust. Soc. Am., *52*, No. 3 (1972), pp. 711–719.
19. W. S. Griffin, H. H. Richardson, and S. Yamanami, "A Study of Fluid Squeeze-Film Damping," J. Basic Engineering, Trans. ASME, *88*, No. 2 (June, 1966), pp. 451–456.
20. K. Teer, "On the Optimum Configuration for a Condenser Microphone," Acoustica, *15*, No. 5 (1965), pp. 256–263.
21. Yu Chen, *Vibrations: Theoretical Methods*, Reading, Mass.: Addison-Wesley, 1966, eq. (1.3.18).
22. F. W. Fraim and P. V. Murphy, "Electrets in Miniature Microphones," J. Acoust. Soc. Am., *53*, No. 6 (June 1973), pp. 1601–1608.

23. L. L. Beranek, *Acoustics*, New York: McGraw-Hill, 1954. Material in both Sections 5.7 and 5.9 was employed.
24. T. T. Wang and S. Matsuoka, unpublished communication to J. C. Baumhauer, Jr., August 1975.
25. J. D. Ferry, *Viscoelastic Properties of Polymers*, New York: John Wiley, 1970, pp. 60–63.
26. During a visit to Northern Electric Co. (now Northern Telecom, Ltd.) in September 1974, author J. C. Baumhauer, Jr. was informed that the concept of high temperature conditioning for the purpose of relaxing stress and obtaining a more controlled stress level was in use by that company.
27. R. A. Schapery, "Stress Analysis of Viscoelastic Composite Materials," J. of Composite Mat., *1*, No. 3 (July, 1967), pp. 228–267.
28. W. Flügge, *Viscoelasticity*, New York: Springer-Verlag, 1975. See Ch. 1.
29. See Ref. 25, Ch. 11.
30. S. R. Whitesell and R. S. Ball, unpublished communication to A. M. Brzezinski in March/October 1977.